Giant Resistance Change across the Phase Transition in Spin-Crossover Molecules

N. Baadji and S. Sanvito

School of Physics and CRANN, Trinity College, Dublin 2, Ireland

(Received 10 January 2012; published 21 May 2012)

The electronic origin of a large resistance change in nanoscale junctions incorporating spin-crossover molecules is demonstrated theoretically by using a combination of density functional theory and the nonequilibrium Green's function method for quantum transport. At the spin-crossover phase transition, there is a drastic change in the electronic gap between the frontier molecular orbitals. As a consequence, when the molecule is incorporated in a two-terminal device, the current increases by up to 4 orders of magnitude in response to the spin change. This is equivalent to a magnetoresistance effect in excess of 3000%. Since the typical phase transition critical temperature for spin-crossover compounds can be extended to well above room temperature, spin-crossover molecules appear as the ideal candidate for implementing spin devices at the molecular level.

DOI: 10.1103/PhysRevLett.108.217201 PACS numbers: 75.30.Wx, 31.15.A−, 73.23.−b, 85.75.−d

The past few years have witnessed several attempts at implementing spin devices at the single molecule level [1–3]. These include spin valves, where organic molecules are used as a transport medium for spin-polarized electrons injected from magnetic metals [4–6], and three-terminal junctions incorporating magnetic molecules [7]. The second strategy appears particularly intriguing, as the electrical response of single molecule magnets depends sensitively on both their spin and charge configuration [7,8]. This sensitivity, combined with the possibility of manipulating the spin state of a molecule by electrical means [9,10], makes spin electronics based on magnetic molecules an attractive platform for both conventional and quantum logic.

There are, however, two unfortunate drawbacks in constructing spin devices based on molecular magnets. The first concerns the typically poor structural stability of such molecules away from solution. For instance, almost all the members of the Mn_{12} family react on metallic surfaces, so that their structural and electronic integrity is uncertain once they are incorporated in a device [11]. The second problem has to do with the magnetic anisotropy. In fact, although the anisotropy density per atom may be very large, the overall magnetic anisotropy of the molecule is rather small, since only a handful of atoms contribute to the magnetic moment. This means that at room temperature the spin quantization axis of the molecule fluctuates at a frequency much higher than the transport measurement time and the molecule appears paramagnetic to a steady state transport experiment. Importantly, while the first problem can be kept under control by engineering the end groups binding to the substrate [12], the second one appears to be much more tough to overcome. In fact, quantum tunneling of the magnetization is always present so that the instability in the magnetization direction may persist down to low temperatures. It is then not surprising that the only demonstration to date of a spin-valve effect originating from molecular magnets is limited to ultralow temperatures [13,14].

One possible way to overcome such a difficulty is to abandon the concept of the spin valve and to look at devices where the information is contained in the actual spin magnitude and not in its direction. A natural choice for such an alternative device concept is that of using molecules displaying a magnetic bistability, i.e., molecules that can be found in two different spin states, both accessible with an external stimulus. This is the realm of spin-crossover compounds [15]. Such materials are formed by $3d$ transition metal ions in an octahedral surrounding, which display a spin transition from a low-spin (LS) state, usually the ground state, to a high-spin (HS) state, usually a metastable one. Such a LS-HS transition can be triggered by temperature, pressure, or light. It is accompanied by a modification of the geometrical structure, which alters the crystal field strength. The most extensively investigated spin-crossover compounds contain Fe(II), and the transition is between a ${}^1A_{1g}$ LS state to a ${}^5T_{2g}$ HS one.

To date, electron transport experiments in spin-crossover molecules at the single molecular level remain scarce, mostly because the effort in depositing such molecules on surfaces has intensified only recently. However, several deposition techniques are becoming available (e.g., Ref. [16]), and a first demonstration of light-induced spin crossover in vacuum-deposited thin films has been already reported [17]. Intriguingly, the critical temperature for spin crossover in such thin films is similar to that of the bulk, giving hope that room temperature device operation may be soon achievable. Also intriguing is the possibility to tune the spin-crossover transition with an electric field, as demonstrated recently for valence tautomeric compounds [18].

Importantly, there are two demonstrations of the interplay between the spin-crossover transition and the electron transport properties of a device. Prins *et al.* [19] measured a change in the current-voltage, I-V, curve of a Fe-$(trz)_3$

(trz denotes triazole) complex deposited between Au nanogap electrodes, which correlates well with the spin-crossover transition. Furthermore, the three-terminal single molecule experiments of Meded *et al.* [20] showed low-energy features attributable to spin crossover and controllable by gating.

A crucial aspect of spin-crossover compounds is that at the LS to HS phase transition there is a simultaneous electronic and structural change of the molecule. The electronic gap between the highest occupied molecular orbital (HOMO) and the lowest unoccupied molecular orbital (LUMO) varies according to the different occupation of the $3d$ multiplet, and at the same time there is an out-breathing relaxation of the octahedral cage connected to the weakening of the crystal field. As such, in transport experiments it is difficult to separate effects arising from the electronic structure from those originating from the molecule geometry. In this Letter, we address such an issue with state of the art electron transport calculations based on density functional theory. In particular, we show that the change in the HOMO-LUMO gap at the phase transition may generate extremely large changes in the I-V characteristic. This is demonstrated for the prototypical Fe(II) SCC $[\mathrm{Fe}L_2]^{+2}$, where L is a 2, 2′:6, 2″-terpyridine group [see Fig. 1(a)]. Note that qualitatively similar results (not presented here) have been obtained for a second $[\mathrm{Fe}L_2]^{+2}$ compound where L is 2,6-bis(pyrazol-1-yl), so that we expect our main conclusions to bear generality.

Calculating the electronic properties of spin-crossover molecules with density functional theory is a rather difficult task, as the relative energy separating the LS and HS states is very sensitive to the choice of exchange and correlation functionals and to the atomic relaxation [21] (note that the molecule atomic coordinates are known only for single crystals but not in vacuum or on a surface). We then use the following strategy. We first perform structural relaxation for the molecule in vacuum by using the Becke three-parameter Lee-Yang-Parr hybrid (B3LYP) functional [22], one of the better performing for this problem. Then the results are compared with those obtained by using the generalized gradient approximation (GGA) and the local density approximation incorporating the self-interaction corrections (LDA-SIC) [23]. From this analysis we select the GGA functional to be used for the electron transport calculations, as this reproduces qualitatively the HOMO-LUMO gap obtained by the B3LYP functional [24].

We start our analysis by discussing the electronic and geometric properties of the molecule in the gas phase. B3LYP calculations are performed with the NWCHEM package [25]. The basis set is 6-31 + $+G^{**}$ for H, C, and N, while for Fe we use the Los Alamos double ζ with an effective core potential [26]. In Fig. 1(c), we present the total energy as a function of the reaction coordinates, X, interpolating between the LS ($X = 0$) and the HS ($X = 1$) geometry for the two different spin configurations. In the same figure, we also show the dependence of the HOMO-LUMO gap, ΔE_g, as a function of X.

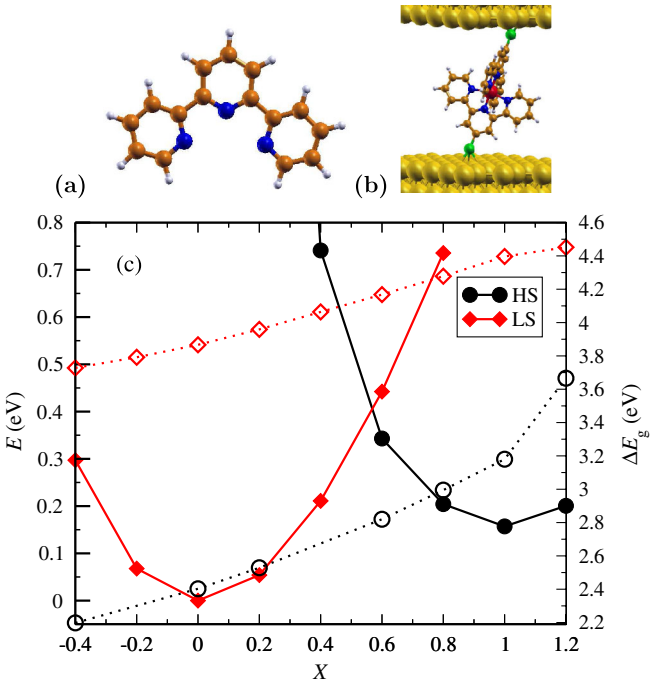

FIG. 1 (color online). Electronic properties of $[\mathrm{Fe}L_2]^{+2}$, $L =$ 2, 2′:6, 2″-terpyridine, along the reaction coordinates X. In (a) and (b) we show, respectively, the 2, 2′:6, 2″-terpyridine group and the cell used for the transport calculations. Color code: C, orange; N, dark blue; H, white; S, green; and Au, yellow. In panel (c) we present the total energy E (full symbols to read on the left-hand side scale) and the HOMO-LUMO gap ΔE_g (open symbols to read on the right-hand side scale) for both LS and HS along X. Calculations are performed with the B3LYP functional.

The figure clearly shows that the ground state is, as expected, low spin. As X increases, there is a transition to high spin for $X \sim 0.6$ with the difference between the energy minima of the two spin configurations being about 200 meV. The HOMO-LUMO gap also changes as a function of X, increasing for both the spin states as one goes from the low- to the high-spin geometry (X gets bigger), i.e., as the ligand field weakens. Most importantly, at the relative energy minimum the gap, calculated with the B3LYP functional, of the LS state is 3.87 eV (for $X = 0$), while that of the HS is only 3.18 eV (for $X = 1$). At the same two energy minima, LDA-SIC [27] gives us HOMO-LUMO gaps of 3.35 (LS) and 2.84 eV (HS), while GGA returns 1.81 (LS) and 0.33 eV (HS). Although different exchange and correlation functionals yield sensibly different gaps, in all cases this contracts significantly across the phase transition. Importantly, both the B3LYP functional and GGA give us spin down HOMO and LUMO levels in the HS state, while with LDA-SIC the HOMO is spin up and the LUMO is spin down. As such, we decide to use GGA instead of LDA-SIC for the transport calculations.

We construct a two-terminal device by attaching the FeL_2 molecule to a Au(111) surface via the thiol group. In particular, we consider bonding to the (111) hollow site, and we optimize the Au-S distance for two different angles between the molecule and the normal to the surface, namely, 0 and 30°. As the transport properties depend weakly on such a tilting angle, the results reported here refer only to the 30° case, the bonding geometry presenting a lower energy. Transport calculations are performed with the SMEAGOL code [28,29], which implements the nonequilibrium Green's function method within density functional theory [30]. The wave function is expanded over a numerical atomic orbital basis set, and the core electrons are described with norm-conserving pseudopotentials including nonlinear core corrections. The basis set has double ζ quality for C, N, H, and Fe, while only single ζ is employed for Au. The simulation cell contains the molecule and five (111)-oriented Au layers with an 8×7 cross section. We use periodic boundary conditions in the direction orthogonal to the transport with a uniform 2×2 k-point sampling and an equivalent mesh cutoff of 400 Ry. The charge density is integrated over 64 energy points along the semicircle and 64 energy points along the line in the complex plane, and 64 poles are used for the Fermi distribution (the electronic temperature is 25 meV). During the finite-bias calculations, we integrate the Green's function over the real axis on a 256-point mesh.

Figure 2 displays the total zero-bias transmission coefficient $T(E; V = 0) = \sum_{\sigma}^{\uparrow\downarrow} T^{\sigma}(E; V = 0)$ as a function of energy for both the LS and HS configurations of the junction (σ labels the spin, $\sigma = \uparrow, \downarrow$). The most striking feature is a radical change of the position of the various resonant peaks as the molecule transits from LS to HS. This is a direct consequence of the rearrangement of the Fe d shell density of state originating from the reduction of the ligand crystal field. In particular, as the crystal field weakens in the HS state, the energy width of the d shell reduces and the peaks become more dense. This effect is particularly dramatic around the Fermi level E_F, where the transport HOMO-LUMO gap shrinks. Recalling here the fact that in the linear response the conductance G is simply given by $G = \frac{e^2}{h} T(E_F; V = 0)$, we can conclude that at the phase transition there is a significant conductance enhancement. One can quantify such an effect by defining the spin-crossover magnetoresistance (SCMR) ratio as $R_{\mathrm{SCMR}} = (G_{\mathrm{HS}} - G_{\mathrm{LS}})/G_{\mathrm{LS}}$. At zero bias we find $R_{\mathrm{SCMR}} = 200\%$, a variation which is certainly measurable. Note that across the phase transition there is no change in the molecule valence charge, so that the effect reported here occurs at an energy scale lower than that needed to observe Coulomb blockade.

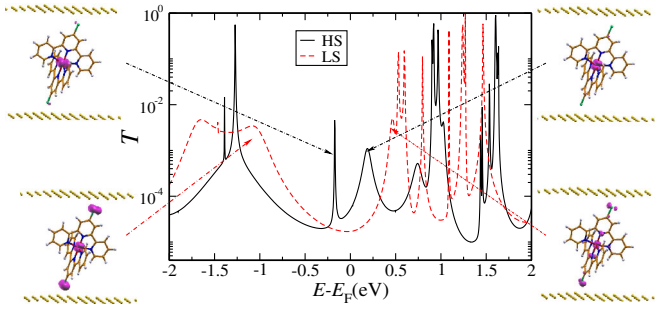

FIG. 2 (color online). Zero-bias transmission coefficient as a function energy, $T(E; V = 0)$, for both the LS (red dashed line) and the HS (solid black line) configuration of the FeL_2-based junction and the molecular orbitals associated to their HOMO- and LUMO-like orbital. Calculations are performed with the GGA functional.

Some more details are provided by the insets in Fig. 2, where we show the frontier molecular orbitals associated to the different peaks in $T(E; V = 0)$. In general, around E_F the orbitals responsible for the transmission have all Fe-d character and mix little with the ligands. In the LS configuration, the HOMO and LUMO are non-spin-polarized and have respectively d_{z^2} and d_{π} character. In contrast, the HS state has a HOMO of $x^2 - y^2$ symmetry, while the LUMO is d_{σ}-like, but both the HOMO and the LUMO are spin down. Thus the gap reduction is the result of the orbital rearrangement of the d manifold associated to the spin-crossover transition. In the LS state, the gap is between the t_{2g} triplet and e_g doublet split by the octahedral crystal field. In the HS configuration, the system undergoes Jahn-Teller distortion in the singly occupied spin down triplet, and thus the gap reduces. Note that such a distortion, and thus the spin-crossover transition, may be obstructed if the molecule is too rigidly bound to the electrodes. As such, for this effect to be detected one has to protect the spin active part of the molecule by appropriate chemical groups, so that the Fe-N cage can deform freely.

Then we look at the I-V characteristics (Fig. 3). Clearly, the drastic gap reduction in the HS state makes its relative current considerably larger than that of the LS. At a voltage of about 0.5 V, the two differ by more than 3 orders of magnitude. The LS current is essentially tunnelinglike over the entire bias window investigated, and it increases monotonically with bias. Such an increase is the result of the enlargement of the bias window, i.e., of the fact that a larger portion of the transmission spectrum contributes to the current. It is then the tail of the LUMO that contributes the most. The HS situation is different, since voltages of the order of 0.4 V are enough for bringing both the HOMO and the LUMO transmission resonances within the bias window (note that orbital rehybridization under bias drifts both the HOMO and LUMO close to each other, hence decreasing the gap). As a consequence, the current grows fast at low bias, when there is a transition from tunneling to resonant transport, and then saturates. Such a large difference in the I-V's of the two spin states translates in a large R_{SCMR}, which is presented as a function of bias in the inset in Fig. 3. Clearly, R_{SCMR} as large as 3000% appear to be possible.

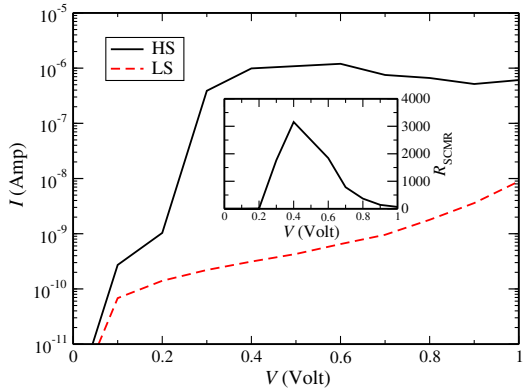

FIG. 3 (color online). I-V curve for a FeL_2 molecule attached to gold electrodes in either the HS (black solid line) or the LS (red dashed line) state. The current is plotted on a logarithmic scale only for positive currents. The inset shows the SCMR ratio R_{SCMR}. Calculations are performed with the GGA functional.

Finally, we look at the effect of a potential gate on the transport properties of the molecule. This is applied by shifting the on-site energies of the molecular orbitals [31]. We note that for both states the transmission spectrum is characterized by a number of relatively sharp peaks spaced by at most 1.5 eV (most typically, the spacing is $\sim$0.3 eV) and corresponding to states with substantial Fe d character. These are expected to shift with bias. As an example, we consider the LS situation, and in Fig. 4 we show $T(E; V = 0)$ as a function of the gate. Here T is plotted as a color code on a logarithmic scale with red corresponding to low transmission (10^{-11}) and blue to high (10^{-1}). Clearly, the entire spectrum shifts with the gate potential until a state,

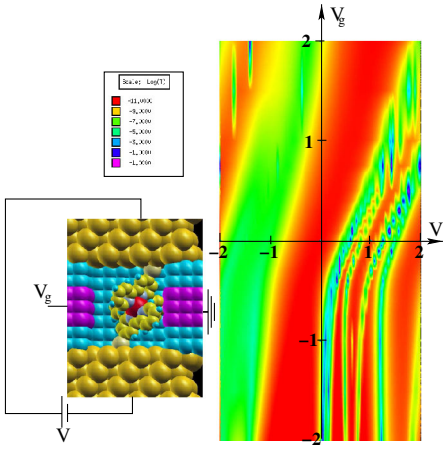

FIG. 4 (color online). Transmission coefficients as a function of energy for different values of the gate potential V_g (molecule in the LS state). Here $T(E; V = 0)$ is plotted as a color code on a logarithmic scale with red corresponding to low transmission (10^{-11}) and blue to high (10^{-1}). In the inset, we show a schematic figure of the device investigated. The purple atoms represent the region in space where the gate is applied. The color code for the atoms is the same as in Fig. 1(b).

either the HOMO or the LUMO, crosses the Fermi level ($V = 0$). At that point, charge transfer takes place and the gate becomes less efficient. Crucially, when one of the two frontier molecular orbitals is brought to E_F, the zero-bias conductance increases dramatically. Since the two spin states of the molecule have different frontier molecular orbitals, their position can be manipulated independently; i.e., they can be brought at E_F for different values of the gate. As such, an extremely large gate-modulated magnetoresistance is expected.

In conclusion, we have demonstrated that the changes in electronic structure associated to the spin-crossover phase transition, namely, the reduction of the HOMO-LUMO gap, produce large changes in the transmission of a two-terminal molecular junction. At low bias we have predicted a spin-crossover magnetoresistance of the order of 200%, which can increase up to 3000% at finite bias. The effect is related to the different nature of the frontier molecular orbitals of the different spin configurations and can be tuned with a gate potential. Such an effect, whose experimental evidence has been already partially provided, can be exploited in the fabrication of spin transistors at the molecular level. Intriguingly, our results not only prove that spins can be manipulated in an organic molecule but also introduce a mechanism for molecular switching which has electronic origin, and it is not associated to a change in the molecule geometry [32].

This work is supported by Science Foundation of Ireland under the NanoSci-E+ project "Internet" (08/ERA/I1759).

[1] S. Sanvito, Chem. Soc. Rev. **40**, 3336 (2011).
[2] L. Bogani and W. Wernsdorfer, Nature Mater. **7**, 179 (2008).
[3] S. Sanvito, J. Mater. Chem. **17**, 4455 (2007).
[4] J. R. Petta, S. K. Slater, and D. C. Ralph, Phys. Rev. Lett. **93**, 136601 (2004).
[5] S. Schmaus, A. Bagrets, Y. Nahas, T. K. Yamada, A. Bork, M. Bowen, E. Beaurepaire, R. Evers, and W. Wulfhekel, Nature Nanotech. **6**, 185 (2011).
[6] C. Barraud, P. Seneor, R. Mattana, S. Fusil, K. Bouzehouane, C. Deranlot, P. Graziosi, L. Hueso, I. Bergenti, V. Dediu, F. Petroff, and A. Fert, Nature Phys. **6**, 615 (2010).
[7] H. B. Heersche, Z. de Groot, J. A. Folk, H. S. J. van der Zant, C. Romeike, M. R. Wegewijs, L. Zobbi, D. Barreca, E. Tondello, and A. Cornia, Phys. Rev. Lett. **96**, 206801 (2006).
[8] C. D. Pemmaraju, I. Rungger, and S. Sanvito, Phys. Rev. B **80**, 104422 (2009).
[9] J. Lehmann, A. Gaita-Arino, E. Coronado and D. Loss, Nature Nanotech. **2**, 312 (2007).
[10] N. Baadji, M. Piacenza, T. Tugsuz, F. D. Sala, G. Maruccio, and S. Sanvito, Nature Mater. **8**, 813 (2009).
[11] M. Mannini, P. Sainctavit, R. Sessoli, C. Cartier dit Moulin, F. Pineider, M.-A. Arrio, A. Cornia, and D. Gatteschi, Chem. Eur. J. **14**, 7530 (2008).

[12] M. Mannini, F. Pineider, C. Danieli, F. Totti, L. Sorace, P. Sainctavit, M. A. Arrio, E. Otero, L. Joly, J. C. Cezar, A. Cornia, and R. Sessoli, Nature (London) **468**, 417 (2010).
[13] M. Urdampilleta, S. Klyatskaya, J-P. Cleuziou, M. Ruben, and W. Wernsdorfer, Nature Mater. **10**, 502 (2011).
[14] S. Sanvito, Nature Mater. **10**, 484 (2011).
[15] P. Gütlich and H. A. Goodwin, in *Spin Crossover in Transition Metal Compounds*, edited by P. Gütlich and H. A. Goodwin (Springer, New York, 2004).
[16] S. Shi *et al.*, Appl. Phys. Lett. **95**, 043303 (2009).
[17] H. Naggert, A. Bannwarth, S. Chemnitz, T. von Hofe, E. Quandt, and F. Tuczek, Dalton Trans. **40**, 6364 (2011).
[18] A. Droghetti and S. Sanvito, Phys. Rev. Lett. **107**, 047201 (2011).
[19] F. Prins, M. Monrabal-Capilla, E. A. Osorio, E. Coronado, and H. S. J. van der Zant, Adv. Mater. **23**, 1545 (2011).
[20] V. Meded, A. Bagrets, K. Fink, R. Chandrasekar, M. Ruben, F. Evers, A. Bernand-Mantel, J. S. Seldenthuis, A. Beukman, and H. S. J. van der Zant, Phys. Rev. B **83**, 245415 (2011).
[21] S. Zein, S. A. Borshch, P. Fleurat-Lessard, M. E. Casida, and H. Chermette, J. Chem. Phys. **126**, 014105 (2007).
[22] A. D. Becke, J. Chem. Phys. **98**, 5648 (1993).
[23] C. D. Pemmaraju, T. Archer, D. Sánchez-Portal, and S. Sanvito, Phys. Rev. B **75**, 045101 (2007).
[24] Note that our electron transport code SMEAGOL at present cannot use nonlocal functionals. Furthermore in general, as far as we know, an implementation of hybrid functions within the nonequilibrium Green's function formalism has not been developed yet.
[25] M. Valiev *et al.*, Comput. Phys. Commun. **181**, 1477 (2010).
[26] P. J. Hay and W. R. Wadt, J. Chem. Phys. **82**, 299 (1985).
[27] Here we set the scaling parameter $\alpha = 0.7$.
[28] A. R. Rocha, V. M. García-Suárez, S. Bailey, C. Lambert, J. Ferrer, and S. Sanvito, Phys. Rev. B **73**, 085414 (2006); Nature Mater. **4**, 335 (2005).
[29] I. Rungger and S. Sanvito, Phys. Rev. B **78**, 035407 (2008).
[30] J. M. Soler, E. Artacho, J. D. Gale, A. García, J. Junquera, P. Ordejón, and D. Sánchez-Portal, J. Phys. Condens. Matter **14**, 2745 (2002).
[31] C. Morari, I. Rungger, A. R. Rocha, S. Sanvito, S. Melinte, and G.-M. Rignanese, ACS Nano **3**, 4137 (2009).
[32] S. J. van der Molen and P. Liljeroth, J. Phys. Condens. Matter **22**, 133001 (2010).